doi.org/10.1002/hlca.202200158

RESEARCH ARTICLE

HELVETICA chimica acta

Solution, Crystal and *in Silico* Structures of the Organometallic Vitamin B_{12}-Derivative Acetylcobalamin and of its Novel Rhodium-Analogue Acetylrhodibalamin

Markus Wiedemair,[a] Christoph Kieninger,[a] Klaus Wurst,[b] Maren Podewitz,*[c] Evelyne Deery,[d] Michael D. Paxhia,[e] Martin J. Warren,[d, e] and Bernhard Kräutler*[a]

[a] Institute of Organic Chemistry & Center for Molecular Biosciences (CMBI), University of Innsbruck, AT-6020 Innsbruck, Austria, e-mail: Bernhard.Kraeutler@uibk.ac.at

[b] Institute of General, Inorganic & Theoretical Chemistry, University of Innsbruck, AT-6020 Innsbruck, Austria

[c] Institute of Materials Chemistry, TU Wien, AT-1060 Vienna, Austria, e-mail: maren.podewitz@tuwien.ac.at

[d] School of Biosciences, University of Kent, Canterbury, CT2 7NJ, UK

[e] Quadram Institute Bioscience, Norwich Research Park, Norwich NR4 7UA, UK

Dedicated to the memory of Professor *Jack D. Dunitz*

The natural vitamin B_{12}-derivatives are intriguing complexes of cobalt that entrap the metal within the strikingly skewed and ring-contracted corrin ligand. Here, we describe the synthesis of the Rh(III)-corrin acetylrhodibalamin (**AcRhbl**) from biotechnologically produced metal-free hydrogenobyric acid and analyze the effect of the replacement of the cobalt-center of the organometallic vitamin B_{12}-derivative acetylcobalamin (**AcCbl**) with its group-IX homologue rhodium, to give **AcRhbl**. The structures of **AcCbl** and **AcRhbl** were thoroughly analyzed in aqueous solution, in crystals and by *in silico* methods, in order to gain detailed insights into the structural adaptations to the two homologous metals. Indeed, the common, nucleotide-appended corrin-ligand in these two metal corrins features extensive structural similarity. Thus, the rhodium-corrin **AcRhbl** joins the small group of B_{12}-mimics classified as 'antivitamins B_{12}', isostructural metal analogues of the natural cobalt-corrins that hold significant potential in biological and biomedical applications as selective inhibitors of key cellular processes.

Keywords: antivitamin B_{12}, cobalt, corrin, density functional calculations, organometallic chemistry, *Salmonella*, rhodium, transition metals, X-ray diffraction.

Introduction

The natural B_{12}-derivatives are important cobalt complexes that encase the metal within a ring-contracted corrin ligand.[1–3] The particular mutual interplay of cobalt and corrin in the B_{12}-cofactors is essential for their fundamental biological functions, which are indispensable in all kingdoms of life.[4] The corrin ligand incarcerates cobalt-ions very tightly,[5,6] and provides a ring-contracted and skewed helical coordination environment for the metal-ion, acting as a unique entatic state module that activates the B_{12}-cofactors for enzyme catalysis.[7] However, the exceptional chemical basis of cobalt for its role in B_{12}-cofactors remains intriguing.[2,8]

In line with studies on metal-analogues of the cobalamins (Cbls)[9–12] we have become particularly interested in gaining access to well characterized rhodium analogues of the natural B_{12}-derivatives, in order to study the effect of the replacement of the

Supporting information for this article is available on the WWW under https://doi.org/10.1002/hlca.202200158

natural cobalt-centers by the homologous transition metal rhodium.[13,14]

As discovered in the course of the comparison of the structures of coenzyme B_{12} (5′-deoxy-5′-adenosylcobalamin, **AdoCbl**) and of 5′-deoxy-5′-adenosylrhodibalamin (**AdoRhbl**), the structural features of the latter suggested the corrin ligand to provide a slightly better fit for the Rh(III)-center, rather than for the natural Co(III)-ion.[9] A similar conclusion resulted from a comparison of the crystal structures of chlorocobalamin (**ClCbl**) and chlororhodibalamin (**ClRhbl**).[12] Most importantly, these previous investigations established largely common coordination-chemical features of the Rh(III)- and Co(III)-ions in Rhbls and Cbls, respectively, and indicated a comparable metal-center mediated (structural and kinetic) trans-influence of the axial ligands.[12]

Herein, we describe acetylrhodibalamin (**AcRhbl**), a previously unknown organometallic Rhbl, prepared by a combination of biological and chemical synthesis steps, and which has been structurally characterized in aqueous solution as well as in a single crystal. We compare the structural and electronic properties of **AcRhbl** with those of the Cbl-analogue acetylcobalamin (**AcCbl**) (see *Figure 1*).[15–18] In both of these organometallic acyl-corrins we observe the acetyl group in an approximate East-West orientation with respect to the metallocorrin moiety. This unprecedented conformational type of a B_{12}-derivative with an unsaturated cobalt-bound carbon center[19,20] stimulated a more fundamental analysis of the organometallic bonding in **AcRhbl** and **AcCbl** by computational means, details of which are also reported herein.

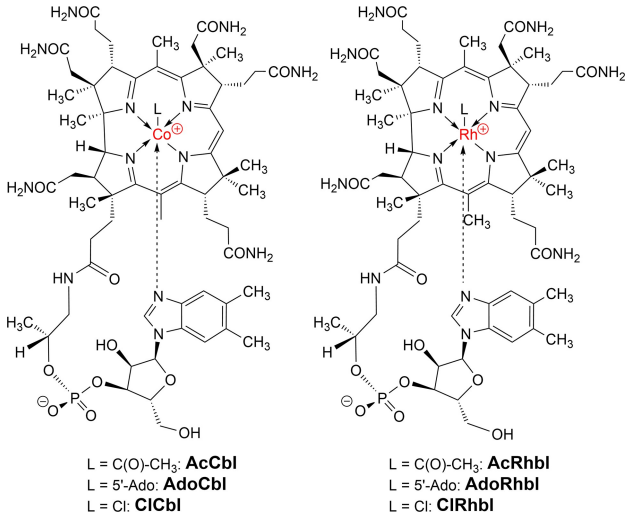

Figure 1. Structural formulae of cobalamins (left) and of rhodibalamins (right).

Results and Discussion

Acetylrhodibalamin (**AcRhbl**) was prepared by attachment of the complete B_{12}-nucleotide[2,21] to the 'incomplete' acetyl-rhodibyrate (**AcRhby**), newly synthesized in two steps from hydrogenobyric acid (**Hby**)[7] (see *Scheme 1*). The terminal condensation reaction of **AcRhby** with the B_{12}-nucleotide was

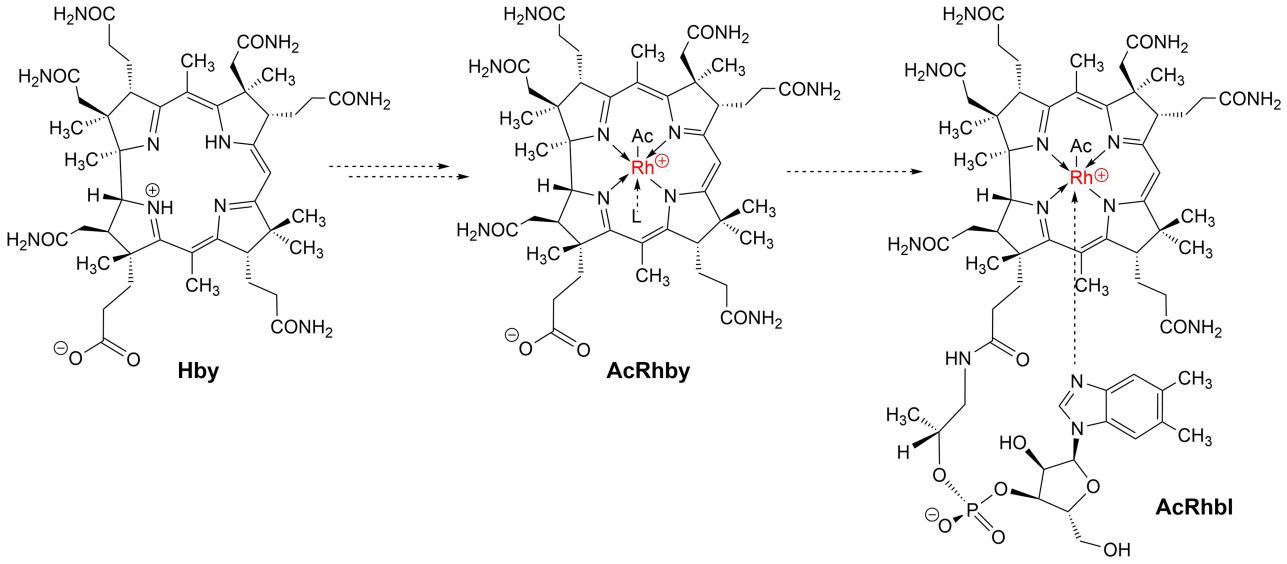

Scheme 1. Structure-based outline of the synthesis of acetylrhodibalamin (**AcRhbl**) from hydrogenobyric acid (**Hby**) *via* Rh-acetylrhodibyrate (**AcRhby**), where L = solvent molecule as potential 'lower' axial ligand.

carried out in aqueous solution following methodology developed for the final step of the partial syntheses of vitamin B_{12} and coenzyme B_{12}, originally,[22] and later also adapted for the total synthesis of the organometallic rhodibalamin (Rhbl) **AdoRhbl**.[9] This methodology exploits the pre-coordination of the B_{12}-nucleotide to the metal-center and the amide-formation at the *f*-propionate side chain in a particularly efficient intramolecular process assembling the nearly strainless 19-membered ring of the 'nucleotide loop', a concept pioneered by *Eschenmoser* in studies on the self-constitution of the Cbls[2] (for details, see [21]). In the present work, this synthesis step furnished crystalline **AcRhbl** in a yield of 58%. The 'incomplete' acetyl-Rh(III)-corrin **AcRhby** was synthesized in high yield by sodium borohydride ($NaBH_4$) reduction of raw chlororhodibyrate in aqueous solution, furnishing a tentatively identified Rh(I)-rhodibyrate intermediate, followed by subsequent acetylation at the presumed highly nucleophilic Rh(I)-center by acetic anhydride (AcOAc). Hence, the typical organometallic and redox chemistry of natural B_{12}-derivatives,[23] exploited in the partial synthesis of acetyl-Co(III)-corrins,[15–18] was employed here for the synthesis of the acetylrhodibyrate **AcRhby** from aquochlororhodibyrate ((H_2O)**ClRhby**). The raw (H_2O)**ClRhby** was prepared in high yield from the metal-free corrin **Hby**, using a methodology that employs the dimeric Rh(I)-complex $[ClRh(CO)_2]_2$ under inert gas, as developed for the synthesis of model Rh-corrins by *Blaser* and *Eschenmoser*,[24] and later adapted by *Koppenhagen et al.* for Rh-incorporation into biologically available metal-free corrins.[25,26]

Serendipitously, under the precise original conditions employed in our lab for Rh(I)-incorporation into the metal-free corrin **Hby**, when acetic acid distilled from phosphorous pentoxide was used as a dry solvent, puzzlingly **AcRhby** was detected as a side product. In order to explore the suspected role of acetic anhydride, generated inadvertently in the distillate, it was found that the deliberate inclusion of a small amount of acetic anhydride in a control experiment led to **AcRhby** as a major product, indicating efficient acetylation of Rh(I)-rhodibyrate. This result also suggested the significance of this potential intermediate from the metallation of **Hby** by $[ClRh(CO)_2]_2$. The attachment of the acetyl group of **AcRhby** occurred with high face-selectivity at the 'upper' β-face of the metal-center, so that covalent conjugation with the B_{12}-nucleotide directly led to the Cbl-homolog **AcRhbl**.

The molecular formula $C_{64}H_{91}N_{13}O_{15}PRh$ of the total-synthetic organometallic Rh-corrin **AcRhbl** was verified by mass spectrometric analysis. Further spectral and crystallographic characterization of **AcRhbl** established its detailed properties (see below and *Supporting Information*). The UV/Vis-spectrum of **AcRhbl** (see *Figure 2*) displays the typical features of the spectra observed with most metallo-corrins through the presence of pronounced α, β and χ-bands with maxima at 502, 482 and 344 nm, respectively. In contrast, acetylcobalamin (**AcCbl**) features an 'atypical' absorption spectrum with broader maxima and lacking a corrin-type band structure (see *Figure 3*). The UV/Vis-spectra of the B_{12}-cofactors methylcobalamin (**MeCbl**) and coenzyme B_{12} (**AdoCbl**) are similarly 'atypical', as are those of most organometallic Co(III)-corrins.[5] The puzzling spectral characteristics of the organocobalamins are a particular sign of the exceptional electronic interactions between the Co(III)-center and the corrin ligand.[27,28] Indeed, the deductions from the UV/Vis-spectral comparison of **AcRhbl** and **AcCbl** reported herein have precedence with the **AdoRhbl** and **AdoCbl** pair of compounds.[9]

The solution structure of **AcRhbl** in water was studied by homo-and hetero-nuclear NMR-spectroscopy at 700 MHz. The data from $^1H,^1H$-COSY and ROESY spectra, as well as from $^1H,^{13}C$-HSQC und HMBC-spectra of **AcRhbl** (in H_2O/D_2O 9:1), allowed the assignment of the signals of all of its 76 non-(exchange)-labile H-atoms, in addition to the 13 amide

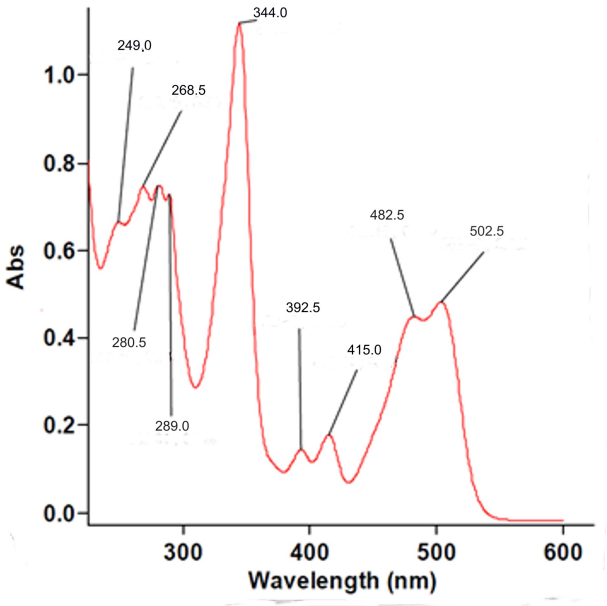

Figure 2. UV-Vis spectrum of **AcRhbl**, $c = 5.23 \times 10^{-5}$ M in H_2O.

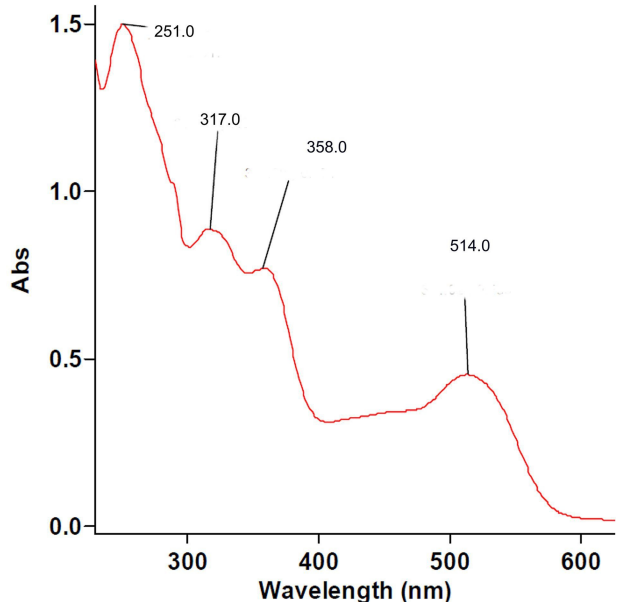

Figure 3. UV-Vis spectrum of **AcCbl**, $c = 7.3 \times 10^{-5}$ M in H_2O.

protons, and of all 64 C-atoms (see *Supporting Information Tables S6* and *S7*). The methyl group *singlet* of the Rh-bound acetyl ligand of **AcRhbl** was observed at 0.77 ppm in the 700 MHz ^{1}H-NMR spectrum (see *Figure 4*), shifted up-field by 1.46 ppm from the resonance of the acetone methyl groups. As deduced from a ^{1}H,^{13}C-HMBC-spectrum, it is spin-coupled with a carbonyl ^{13}C-atom at 235.3 ppm. Analysis of ^{1}H,^{1}H-NOE-spectra verified the base-on nature of **AcRhbl** and the β-configuration of the Rh-bound acetyl group (see *Supporting Information Figure S24*). Furthermore, it suggested an extensive re-orientational mobility of the organometallic acetyl group, primarily residing in an East-West orientation with the acetyl-methyl close to the hydrophobic top face of the ring *C*-moiety. However, according to the observed NOE-correlations, the acetyl group also explored orientations that placed its methyl group close to $H_2C(71)$ at ring *B* and, in the opposite direction, towards $H_3C(17B)$ and HC(19) at ring *D*, but not close to ring *A*.

Acetylcobalamin (**AcCbl**) was prepared from aquacobalamin chloride (**H_2OCbl·Cl**) applying the previously established method of acetylation of the reduced cob(I)alamin,[15,16,18] using acetic anhydride. **AcCbl** was fully characterized, including homo- and heteronuclear NMR spectroscopy in H_2O/D_2O (9:1). Based on the NMR data of **AcCbl** the signals of all of its 64 C-atoms could be assigned, as well as of all of its 76 non-(exchange)-labile H-atoms, in addition to the 13 amide protons (see *Supporting Information*, *Tables S3* and *S4*). In a 700 MHz ^{1}H-NMR spectrum of **AcCbl**, the acetyl group gave rise to a methyl group *singlet* at 1.37 ppm, downfield by 0.60 ppm from the position of the acetyl methyl in **AcRhbl** (see *Figures 4* and *5*). A ^{1}H,^{13}C-HMBC-spectrum revealed it to spin-couple with a carbonyl^{13}C-atom at 241.7 ppm.

The comparison of the chemical shifts of corresponding nuclei in **AcRhbl** and **AcCbl** (see *Supporting Information*, *Figures S25* and *S26*) confirmed the very similar solution structure of the two homologous metal-corrins. However, significantly different electronic interactions of the metal cores with their directly bonded ligand-atoms were indicated. Further analysis has also revealed minor structural differences located

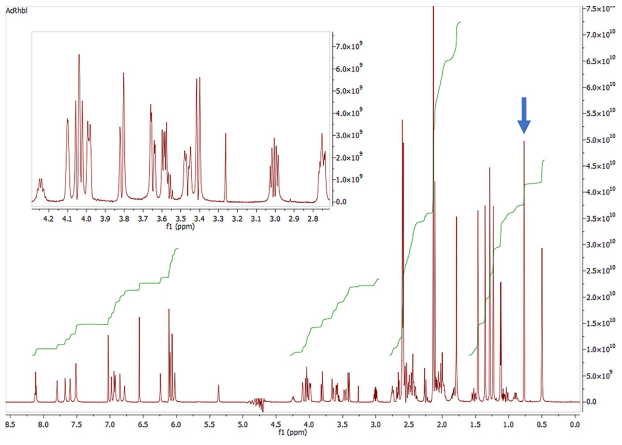

Figure 4. 700 MHz ^{1}H-NMR-spectrum of **AcRhbl** (298 K, KP6-buffer H_2O/D_2O 9:1, $c = 2$ mM). Insert: enlarged portion of the spectrum at intermediate field (blue arrow marks acetyl-methyl signal).

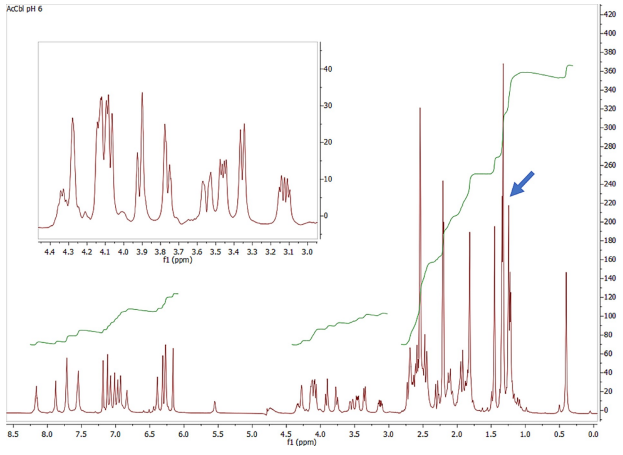

Figure 5. 700 MHz ^{1}H-NMR-spectrum of **AcCbl** (298 K, KP6-buffer H_2O/D_2O 9:1, $c = 2$ mM). Insert: enlarged portion of the spectrum at intermediate field (blue arrow marks acetyl-methyl signal).

at the 'lower' face, which we ascribe to a slightly different nucleotide loop architecture in the cobalt-corrin **AcCbl** *vs.* the Rh-analogue **AcRhbl**. Hence, the NMR data suggest closely related structural properties of the acetyl-Co(III)- and acetyl-Rh(III)-corrins **AcCbl** and **AcRhbl**, including an exceptional preferred East/West-orientation of their organometallic acetyl ligand (see *Supporting Information*, *Figures S4* and *S24*, *Table S9*). However, when comparing the ^{1}H-NMR data for the 'incomplete' Rh-corrin **AcRhby** and the protonated base-off form **HAcCbl**$^{+}$ of the cobalt-corrin **AcCbl** signals of several corresponding H-atoms at the cobalt-corrin moiety display more pronounced chemical shift differences. These could relate, for instance, to different axial coordination in 5-coordinate protonated **HAcCbl**$^{+}$ and 6-coordinate **AcRhby** due to the absence or presence of ligated solvent molecules at the lower face of the metal-centers. Alternatively, the protonated and de-coordinated DMB-nucleotide of **HAcCbl**$^{+}$ might still exert significant anisotropic effects at the lower face of the corrin moiety, as found in ^{1}H-NMR spectra of hydrogenobalamin, the complete metal-free ligand of vitamin B_{12}.[11]

In the UV/Vis-spectrum of the 'incomplete' organometallic Rh-corrin **AcRhby**, the α, β and χ-bands occur at 481, 462 and 336 nm, respectively (see *Supporting Information*, *Figure S19*), *i.e.*, at wavelengths significantly shorter than in the spectrum of **AcRhbl**, where the coordination of the DMB caused bathochromic shifts. The calculated molecular formula of **AcRhby** ($C_{47}H_{67}N_{10}O_9Rh$) was confirmed by an ESI-mass spectrum, in which the *pseudo*-molecular ion $[M+H]^{+}$ was at $m/z = 1019.42$ (see *Supporting Information*, *Figure S15*). In a 700 MHz ^{1}H-NMR spectrum of **AcRhby** in D_2O, the chemical shifts of the *singlet*s at 6.42 ppm and 0.74 ppm allowed their assignment to the corrin methine HC(10) and to the acetyl methyl, respectively. The up-field shift of the signal of the acetyl methyl group of **AcRhby** was merely 0.03 ppm greater than for **AcRhbl** (see below and *Supporting Information Figures S20* and *S23*).

The isolate from the incorporation of rhodium into the metal-free corrin **Hby** behaved as a slowly interconverting mixture of two only partially characterized chlororhodibyrates. When separated by HPLC the two main fractions appeared to contain a (apparently more polar) dichlororhodibyrate (**Cl$_2$Rhby**) and a single (apparently less polar) aquochlororhodibyrate isomer, (H_2O)**ClRhby**. Both were provisionally characterized on the basis of their UV/Vis-spectra. Consistent with this tentative assignment, the isolated (H_2O)**ClRhby** slowly coordinated a second chloride ion in 5 M aqueous NaCl at room temperature, which was selectively lost at ambient temperature in dilute chloride free aqueous solution (see *Supporting Information*, *Figures S10–S13*).

Single crystals of **AcRhbl** and of **AcCbl**, were grown from water/acetonitrile mixtures at room temperature, allowing for well-resolved, cryotemperature X-ray crystal structures of both compounds (see *Supporting Information*). The two homologous 'complete' corrins, **AcRhbl** and **AcCbl**, crystallized in the orthorhombic space group $P2_12_12_1$, with four solvent separated corrinoid molecules per unit cell. The crystal structures of **AcRhbl** and **AcCbl** confirmed their NMR-derived chemical constitutions and furnished precise insights into the bonding around both metal-centers, the corrin ligand conformation and the preferred orientation of the acetyl group with respect to the corrin ring (*Figures 6* and *7*).

The homologous Rh- and Co-corrins **AcRhbl** and **AcCbl** have very similar qualitative structural properties, including the unprecedented predominant East/West-orientation of their organometallic acetyl ligands. In fact, in the crystal of **AcCbl** the acetyl group and the acetamide side chain attached to C(2) at ring *A*, both show some disorder (see *Supporting Information*, *Figure S41*). The average orientation of the acetyl-acyl-plane, close to the N(1)–Co–N(3) diagonal results from an orientational disorder by an angle of about 49°, suggesting dominating contributions of non-bonding interactions as external factors, in addition to weak inherent conformational preferences. For **AcRhbl** the orientation of the acetyl group in an approximate

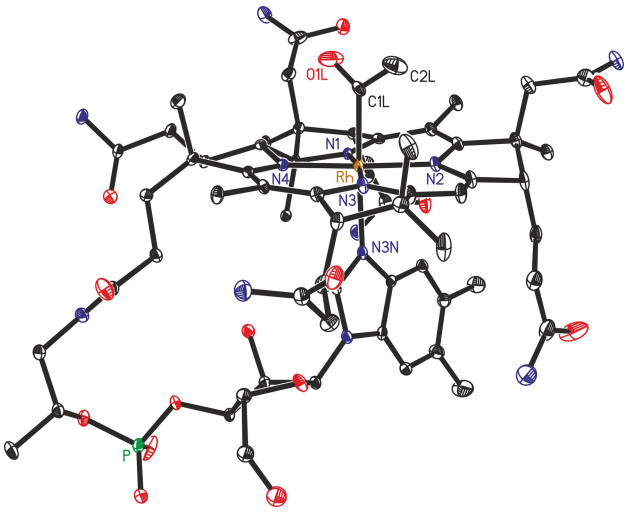

Figure 6. ORTEP-representation of the crystal structure of **AcRhbl** with color coded heteroatoms (red = oxygen, blue = nitrogen, green = phosphor, brown = rhodium).

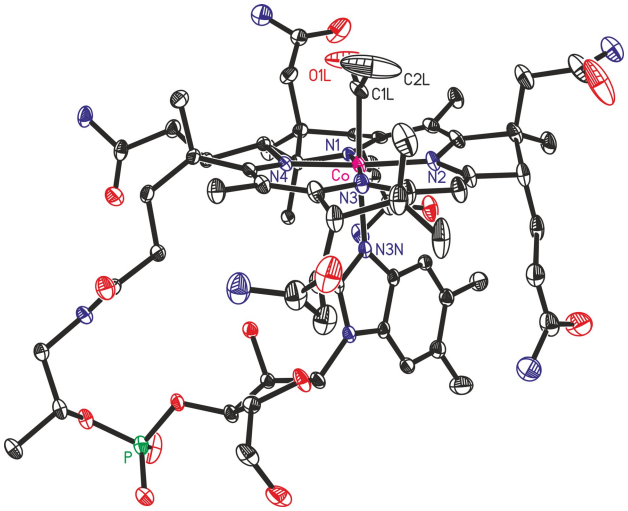

Figure 7. ORTEP-representation of the crystal structure of **AcCbl** with color coded heteroatoms (red = oxygen, blue = nitrogen, green = phosphor, pink = cobalt).

East/West orientation is better defined crystallographically (see *Supporting Information*, *Figure S40*).

The hexacoordinate Rh(III)- and Co(III)-centers of **AcRhbl** and **AcCbl** display a common coordination pattern. Both metal-ions sit in the center of an unsymmetrical, deformed octahedron, spanned by the four inner N-atoms of the helical corrin ligand (arranged as a squashed tetrahedron) and the two axial groups. The six metal-coordinating bonds in **AcRhbl** were roughly 72 mÅ longer (onaverage) than in **AcCbl** (see *Figure 8*). This bond length difference is remarkably close to the difference of 60 mÅ of the covalent radii of Rh(III) and Co(III),[29] suggesting little differential strain in the two organometallic acetyl-corrins. All the equatorial Rh–N bonds and the longer axial bonds had remarkably comparable lengths as in **AdoRhbl**.[9] The Co–C_{sp2} bond in **AcCbl** is slightly longer than in vinyl-cobalamin,[30] but shorter than in an aryl-cobalamin,[20] suggestive of insignificant conjugative or steric effects on the length of the Co–C_{sp2} bond of **AcCbl**.

The mutual structural adaptation of the ligand and the metal-centers has been studied in order to understand better the critical 'fit' of the bound metal-ions with respect to the tetrapyrrolic equatorial ligands.[31] For cobalt-corrins and transition metal analogues, the corrin fold angle,[32] corrin helicity[7] and the deviation from an in-plane arrangement of the inner corrin N-atoms around the metal-centers[11] have been established as important parameters. Their values from the crystal structures of **AcRhbl** and **AcCbl** (see *Table 1*) were all slightly smaller for the Rh(III)-corrin than for the Co(III)-corrin. The slightly smaller corrin-fold angle observed in **AcRhbl** compared to **AcCbl** (13.4° *vs.* 15.6°) may be considered an indication of a somewhat 'better fit' of the Rh(III)-center that is also better able to force the six coordinating atoms into a position closer to the preferred octahedral pattern. However, the interdependence between the corrin-fold angle and the length of the axial bond from the metal center to the DMB-nitrogen, known from extensive correlation in Cbls,[33–35] would also be in line, qualitatively, with a larger fold angle in **AcCbl**, where the Co–N bond is significantly shorter than in **AcRhbl** (see *Figure 8*).

In order to gain further insights into the exceptional conformational characteristics of the acetyl-corrins **AcCbl** and **AcRhbl** and for a better understanding of their structural differences, computational studies of the

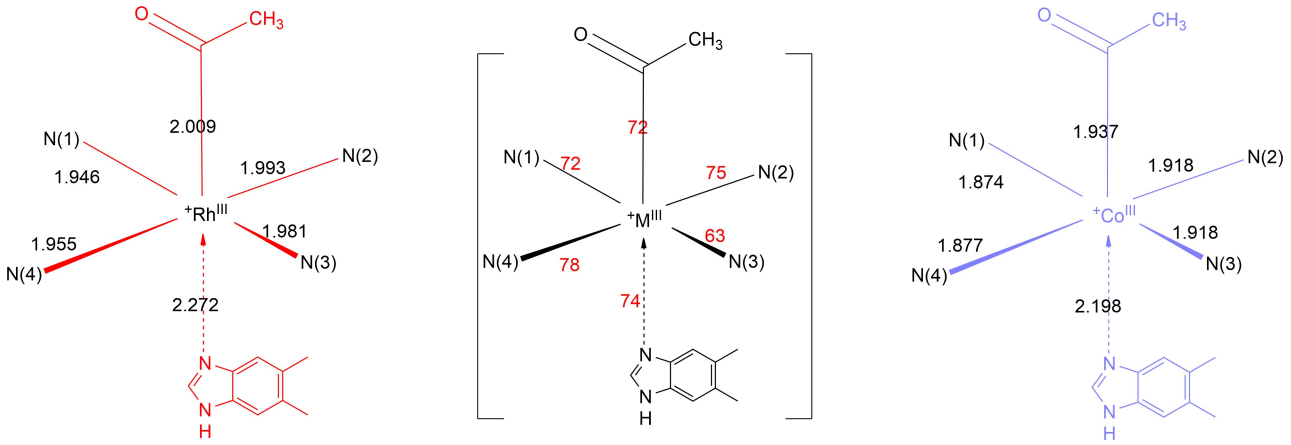

Figure 8. Lengths of coordinating bonds (in Å) around the Rh(III)-center in **AcRhbl** (left), around the Co(III)-center in **AcCbl** (right), as derived from the crystal structures, and differences of these bond lengths in mÅ (middle).

Table 1. Comparison of key structural parameters of **AcCbl** and **AcRhbl** calculated from X-ray crystal structure data.

	AcCbl	AcRhbl
Corrin-fold[32]	15.6°	13.4°
Corrin-helicity[7]	5.1°	3.3°
Nonplanarity at metal-center[11]	5.6°	4.0°
M–C(β) bond length	1.937 Å	2.008 Å
M–N(α) bond length	2.198 Å	2.271 Å
Distance **N(1)–4 N-plane**[a]	−0.068 Å	−0.045 Å
Distance **N(2)–4 N-plane**	+0.059 Å	+0.040 Å
Distance **N(3)–4 N-plane**	−0.059 Å	−0.040 Å
Distance **N(4)–4 N-plane**	+0.067 Å	+0.045 Å
Distance **M-4 N-plane**	+0.014 Å	+0.023 Å

[a] 4 N-Plane denotes the median plane constructed with the positions of the central four coordinating N-atoms. Positive distance values denote a position above (β-side of) the 4 N-plane, negative values a position below, at the α-side.

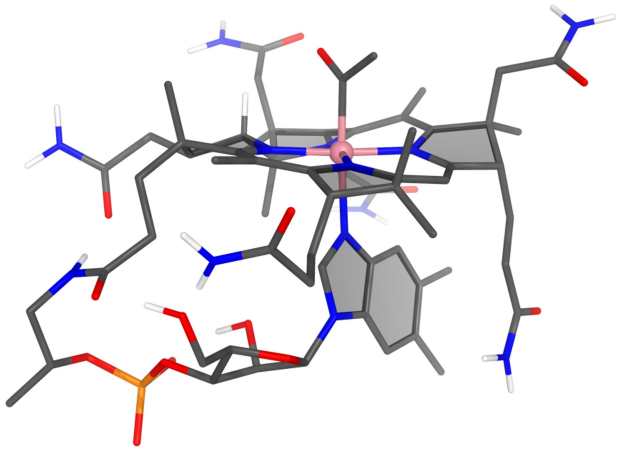

Figure 10. Calculated structure of **AcCbl** (optimized with BP86/def2-SVP/D3 in water); color coded heteroatoms (red = oxygen, blue = nitrogen, white = hydrogen, orange = phosphor, pink = cobalt).

two organometallic acyl-metal complexes were carried out with density functional theory (BP86/def2-SVP/D3) in implicit water. The calculations produced structures of **AcCbl** and of **AcRhbl**, remarkably similar to each other and to the structures from the respective X-ray crystal analyses (see *Figures 9* and *10*). First-of-all, this similarity included the calculated preferred orientation of the axial acetyl-ligand in both structures. Indeed, the calculated bond lengths also followed the crystallographically observed values, all reflecting the basic differences expected for a Co(III)-corrin and a homologous Rh(III)-corrin due to the differing size of these group-IX metal ions[29] (see *Figure 8*). The corrin helicity,[7] 'non-planarity'[11] at the 6-coordinate metal centers and the tetrahedral distortion of the coordinating four N-atoms of **AcRhbl** and **AcCbl** were all calculated as slightly smaller for the Rh(III)-corrin **AcRhbl** than for the Co(III)-corrin **AcCbl** (*Tables 1* and *2*), in line with the crystallographic results.

A small difference was also derived for the corrin fold angle,[32] which was calculated as slightly larger in

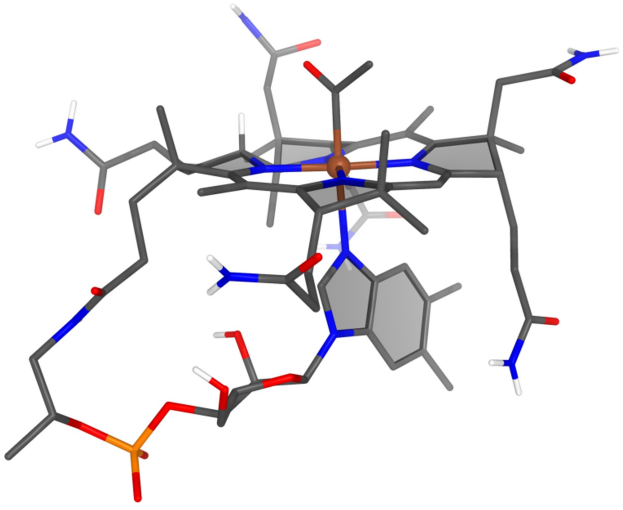

Figure 9. Calculated structure of **AcRhbl** (optimized with BP86/def2-SVP/D3 in water); color coded heteroatoms (red = oxygen, blue = nitrogen, white = hydrogen, orange = phosphor, brown = rhodium).

Table 2. Comparison of calculated structural parameters of **AcCbl** and **AcRhbl**. Optimizations were performed with BP86/def2-SVP/D3 in water.

	AcCbl	AcRhbl
Corrin-fold[32]	15.6	16.4°
Corrin-helicity[7]	6.2°	4.6°
Nonplanarity at metal-center[11]	7.2°	6.0°
M–C(β) bond length	1.922 Å	2.008 Å
M–N(α) bond length	2.146 Å	2.262 Å
M–N(1)	1.867 Å	1.948 Å
M–N(2)	1.920 Å	1.998 Å
M–N(3)	1.927 Å	1.998 Å
M–N(4)	1.870 Å	1.953 Å
Distance **N(1)–4 N-plane**	−0.084 Å	−0.065 Å
Distance **N(2)–4 N-plane**	+0.073 Å	+0.056 Å
Distance **N(3)–4 N-plane**	−0.072 Å	−0.056 Å
Distance **N(4)–4 N-plane**	+0.083 Å	+0.064 Å
Distance **M–4 N-plane**	+0.030 Å	+0.040 Å

4 N-plane denotes the median plane constructed with the positions of the four coordinating N-atoms. Positive distance values denote a position above (β-side of) the 4 N-plane, negative values a position below, at the α-side.

AcRhbl (16.4°) than in **AcCbl** (15.4°), in contrast to the crystallographic result (see *Tables 1* and *2*). However, the arrangement of the nucleotide loop and the orientations and interactions of the polar outer amide functions may cause the small differences concerning the corrin fold angle.

Remarkably, the calculations reproduced the preferred approximate 'West' orientation of the (O-atom of the) acetyl group in both compounds, while also revealing local energy minima for **AcRhbl** and **AcCbl** in the opposite 'East' orientation and, for **AcRhbl**, an additional one in the 'South'. Furthermore, they furnished low global and local conformational energy barriers with respect to the rotation of the acetyl group around its organometallic bond. These were calculated to amount to less than about 28 kJ/mol (or 7 kcal/mol) and18 kJ/mol (or 4.5 kcal/mol) for **AcCbl** and **AcRhbl**, respectively (see *Figure 11*). Hence, the conformational dynamics and orientational preferences of the acetyl-group deduced from the NOE-interproton correlations in 700 MHz ^{1}H,^{1}H-ROESY spectra (see *Supporting Information*, *Figures S7* and *S24*) were fully corroborated by the calculations.

The calculations dismiss the relevance of orientational preferences due to large π-conjugative interactions between (either of) the transition metal centers and the organometallic π-acceptor acyl groups. In fact, further computational investigations of the non-covalent interactions[36,37] between the metal-corrin and acetyl moieties revealed weak attractive interactions in both compounds between the acetyl oxygen and the *a*-acetamide methylene-group ($H_2C(21)$), as well as between the acetyl H_3C-group and the π-system of the corrin ring (see *Supporting Information*, *Figures S42ff*). In the case of **AcCbl**, minor repulsive (steric and closed shell) interactions are indicated at N(2) and N(4) (see *Supporting Information*, *Figures S42* and *S47*). The weak non-covalent interactions and steric effects exerted by the helical and folded corrin ligand and its 'upper' substituents appear to be the main determinants for the preferred conformation(s) of the acetyl group. In **AcCbl** and **AcRhbl**, such interactions may specifically destabilize the 'North/South' orientation of the organometallic ligand that has previously been observed for aryl-Cbls[20,38] and vinyl-Cbls.[30] Furthermore, the preferred orientation of the 'dipolar acetyl rotor', carbonyl oxygen near ring *A* and methyl group near ring *C*, reflects the complementary interfacial polarity at the 'upper' corrin surface, where ring *C* carries a methyl and ring *A* the *a*-acetamide group.

Conclusions

The enduring quest for rationalizing Nature's selection of cobalt for the biologically important corrinoid B_{12}-cofactors[2,3,8] has stimulated a fundamental interest in preparing and studying transition metal analogues of B_{12},[9–12] a long-standing challenge in the B_{12}-field.[26,39,40] Here the specific case of a total biological and chemical synthesis of acetylrhodibalamin (**AcRhbl**) is described, representing the novel rhodium homologue of the known B_{12}-derivative acetylcobalamin (**AcCbl**), together with a detailed structural comparison between this pair of Rh(III)- and Co(III)-corrins. Taken together, the comparison of **AcRhbl** and **AcCbl**, along with two other pairs of corresponding Rhbls and Cbls,[9,12] has suggested a slightly 'better fit' of Rh(III)-ions for the corrin ligand in comparison to Co(III)-ions. However, such comparisons have also shown that rhodium is no match for cobalt, when bound to the natural corrin ligand,[2,7] in terms of providing the biologically essential organometallic reactivity and redox properties of the B_{12}-cofactors.[23] Indeed, the exceptional chemical features of the cobalt-corrins are due to the particular electronic interactions between the bound cobalt-ions and the natural corrin ligand, which also manifest themselves in the 'atypical' absorption spectra of the organometallic B_{12}-cofactors and in their specific photochemical reactivity.[41,42]

The acetyl-corrins discussed herein were selected for the expected σ- and π-bonding properties of the organometallic acetyl group. In fact, **AcCbl** likely lacks any biological catalytic function, and therefore, is a poorly investigated B_{12}-analogue. Earlier hypotheses considered that **AcCbl** may be a key intermediate in the important acetyl-CoA pathway of carbon dioxide fixation of acetogenic and methanogenic microorganisms,[16,43–46] but these ideas have found no experimental support.[47,48] However, the capacity of **AcCbl** and related acyl-cobalamins to serve as light-activated sources of the nucleophilic acyl radicals,[49] may qualify such vitamin B_{12}-derivatives as bio-similar initiators of olefin-polymerization, which is a technology applied nowadays in dental medicine.[50] Preliminary photochemical experiments with **AcRhbl**, indicated that this Rh-homologue of **AcCbl** decomposes very slowly in the presence of air and provided no evidence for photo-induced Rh–C bond cleavage (see *Supporting Information* and *Figures S28–S32*).

Rhodibalamins (Rbls) hold significant potential as antivitamins B_{12},[13,14,51] or as specific B_{12}-antimetabolites,[26,52,53] and, in this regard, the function of **AcRhbl** requires further investigation within a

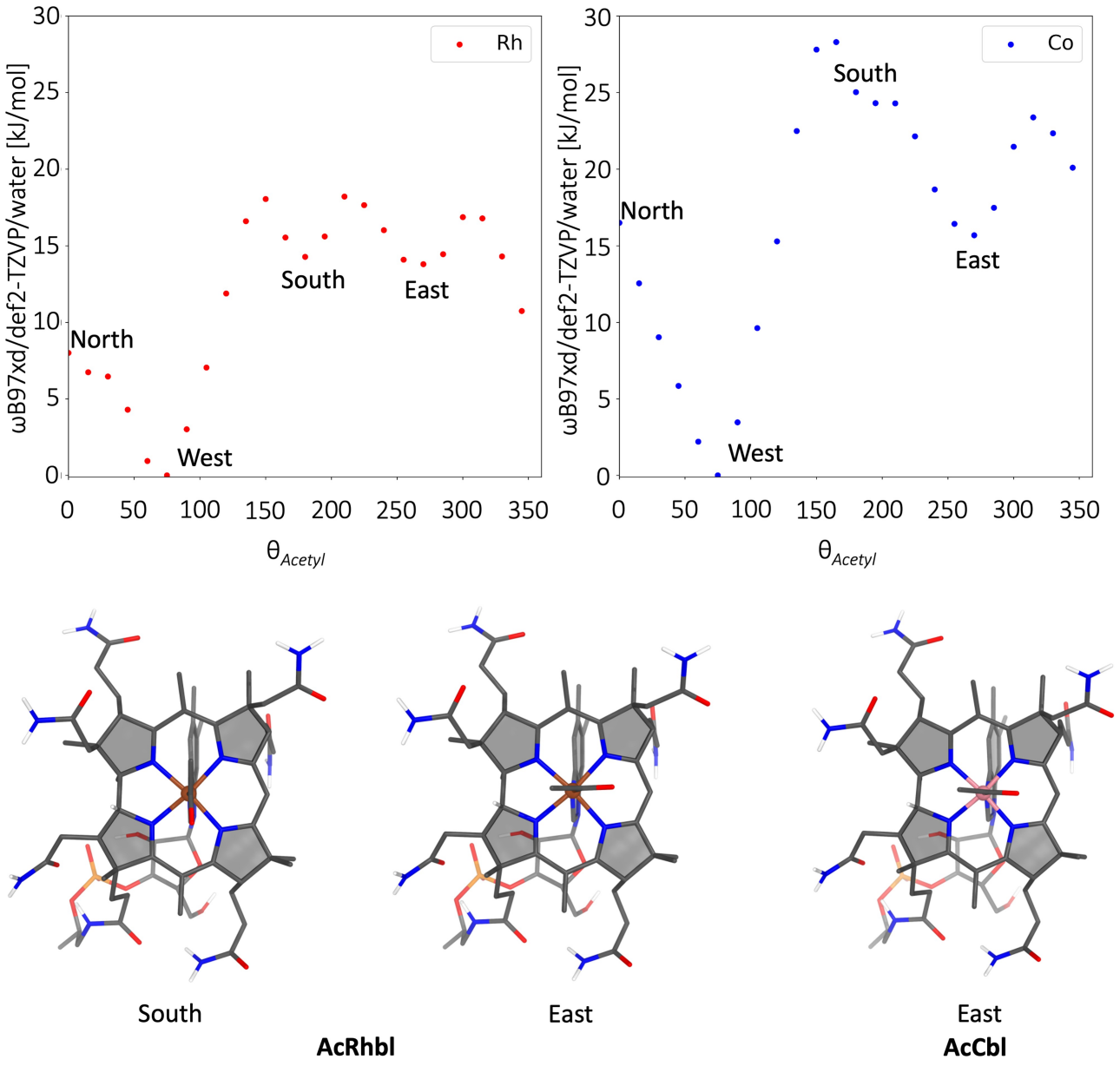

Figure 11. Top: Energy diagrams of the orientation of the acetyl group with respect to the corrin ring in **AcRhbl** (left) and in **AcCbl** (right), depicting global minima for **AcRhbl** and **AcCbl** as 'Western' orientations of the acetyl group, as similarly observed in the respective crystal structures. The dihedral step-size of 15° resulted in 24 structures; each structure was partially optimized with BP86/def2-SVP/D3 in water, while final single point energies were obtained with ω-B97XD3/def2-TZVP, again in water. The dihedral of the orientation 'North' (of the O-atom of the acetyl group) was chosen as reference and set to zero. Bottom: structural models of (local) minimum energy conformers of **AcRhbl** (left) and **AcCbl** (right).

biological context. In this respect, the biological activity of **AcRhbl** underwent exploratory tests using a *Salmonella enterica* B_{12} auxotroph that relies on a B_{12}-dependent methionine synthase for growth on minimal media.[54] As observed with **AdoRhbl**,[9] the bioassay indicated that **AcRhbl** was actively imported by the bacteria and produced inhibitory growth effects. These observations indicate that **AcRhbl** interferes with bacterial metabolism, most likely by impairing the B_{12}-riboswitch regulated import of **CNCbl**.[55,56] In this scenario **AcRhbl** may regulate the riboswitch either directly, or indirectly as a possible metabolic precursor[57] to **AdoRhbl**, the structural **AdoCbl**-mimic. Further studies are planned to elucidate more precisely the inhibitory mechanism considered here.

The close structural similarity with corresponding Cbls is a key criterion[13] for the effective up-take and cellular transport of structural B_{12}-mimics by the critical B_{12}-binding bio-macromolecules in humans[58–60] and other B_{12}-dependent organisms.[61–63] Whereas the acetyl-group of the photo-labile **AcCbl** is rather reactive towards (even mild) nucleophiles,[64] impairing resilience in biological environments, the more photo-stabile **AcRhbl** may also be more resistant to the removal of its acetyl group, since Rh–C bonds are comparatively strong, as seen, *e.g.*, in methyl-Rh(III)-porphyrins.[65] In consequence, **AcRhbl** may be specifically suitable for targeting, *e.g.*, the B_{12}-tayloring glutathione-dependent enzyme CblC in humans and animals that Cbl-based antivitamins B_{12} characteristically inhibit,[20,51,66,67] thus, undercutting the removal of the 'upper' Cbl-ligands that is critical for the metabolic formation of the B_{12}-cofactors.[60,68]

Our structural work has further verified the predicted strong similarity of the coordination-chemical features of the Rh(III)- and Co(III)-centers of corresponding Rhbls and Cbls, respectively, including the unique specific structural *trans*-effect characteristic of the Co(III)-ions, which have been studied in a range of synthetically accessible, inorganic and organometallic B_{12}-derivatives.[3,33] As was observed here for the case of the chlororhodibyrates, and as far as can be deduced more broadly, axial ligand exchange is much slower in Rh(III)-corrins compared to corresponding Co(III)-corrins, which feature fast exchange kinetics of their 'inorganic' axial ligands.[5] Consistent with their evidently stronger bonding, in contrast to the corresponding Co(III)-corrins, Rh(III)-centers appear to be remarkably more effective in imposing a nearly octahedral arrangement on the directly metal-binding atoms of the skewed, helical corrin ligand. As with other antivitamins B_{12},[66] the Rh-mimics of the B_{12}-cofactors hold promise as useful dopplegangers in B_{12}-related biological and bio-structural studies.

Our concerted biological and chemical synthesis approaches to **AcRhbl** and to other transition metal analogues of the cobalamins, or metbalamins (**Metbls**),[9–12] provides an efficient path to the exciting though still hardly explored territory of metallocorrinoids[26,40] and to promising novel biological and biomedical applications.[51,53] As close structural B_{12}-mimics with significantly altered chemical reactivity, the rhodium analogues of the vitamin B_{12} derivatives deserve particular attention as remarkable chemical-biological tools in the multifaceted B_{12}-field. As potential antivitamins B_{12}[14] they are expected to impair the known physiological effects of the vitamin B_{12} forms – as well as still elusive ones – in the metabolism of mammals, potentially giving them key roles in B_{12}-related medical diagnosis and treatment. Their growth-inhibiting effects in B_{12}-dependent organisms, from microorganisms to humans, classify antivitamins B_{12} as antibiotics and as potential anticancer agents, highlighting them as promising pharmaceuticals with a precise, activity targeting structure-based design.

Experimental Section

General

All experimental work was carried out with extensive protection from light. RV: rotatory evaporator (operated at a bath temperature of 40 °C, if not stated otherwise). Desalting: the (mostly aqueous) solution of an isolate was absorbed on *RP18* cartridge and washed with 10 ml of water, followed by MeOH to elute the colored compound(s). See the *Supporting Information* for further experimental details, abbreviations, chromatography, spectroscopy, X-ray crystallography, computation and bioactivity tests, as well as specifications for solvents and reagents.

Synthetic Procedures and Spectral Characterization (for more details, see *Supporting Information*)

Preparation of Acetylcobalamin (**AcCbl**)

AcCbl was prepared from aquocobalamin following the method by *Müller* and *Müller*,[15] but using AcOH/H_2O (1 : 9 *v/v*) as solvent and an *RP18* cartridge for purifying raw **AcCbl** (see *Supporting Information*, *S4* for details). For crystallization, a solution of the purified **AcCbl** in about 1 ml of water was treated with about 3 ml of acetone to give a slightly turbid mixture, which was placed into a refrigerator (10 °C). Red crystals grew overnight and were separated from the mother-liquor, washed with a copious amount of acetone and dried under HV, furnishing 14.4 mg (10.5 μmol, 72 %) of red crystalline **AcCbl**. The sample of **AcCbl** was identified by UV/Vis-, ESI-MS- and ^{1}H-NMR spectra, and characterized further by high field homo-and hetero-nuclear NMR of solutions at pH 6 (base-on form) and pH 2 (protonated base-off form), as well as by CD- and IR-spectra.

Synthesis of Chlororhodibyrate

In a 50 ml *Schlenk* tube dried purified **Hby** (14 μmol) was dissolved in 1 ml of acetic acid and dried again first on an RV, and under HV/r.t. subsequently in order to remove residual solvents. Then the tube was flushed with Ar and the residue was dissolved in 20 ml acetic acid and 20 ml ^{t}BuOH. 100 mg (1.22 mmol, 85.2 equiv.) of anhydrous sodium acetate and 70 mg (0.18 mmol, 12.6 equiv.) of $[ClRh(CO)_2]_2$ were added and was degassed through five cycles of freeze, evacuate (HV) and thaw under Ar. The resulting solution was stirred at r.t. for 43 h, diluted with 200 ml aqueous 150 mm NaCl under air and stirred for 20 min. Then, the solution was concentrated to about 50 ml on an RV and loaded onto a 5 g *RP18* cartridge. The adsorbate was washed with 50 ml of water and eluted with 15 ml of MeOH. An HPLC analysis indicated quantitative conversion and formation of two major chlororhodibyrate fractions. The residual solution was loaded onto a silica column (4×15 cm) and the adsorbate was washed with 200 ml of MeOH. The orange main product fraction was eluted with 92 ml MeOH saturated with NaCl. The eluate was concentrated on an RV, desalted and eluted from the *RP18* cartridge with 10 ml of MeOH. The product solution containing roughly 11.6 μmol (analyzed by UV-Vis, about 82% yield) of a roughly 1:1 mixture of the chlororhodibyrates, tentatively identified by HPLC (see *Supporting Information*, *Figure S11*) as dichlororhodibyric acid (**Cl_2Rhby**) and (a single isomer, mainly, of) aquochlororhodibyrate (H_2O)**ClRhby**. This isolate was evaporated on an RV and the residue was dried under HV. UV-Vis ((H_2O)**ClRhby**, in about 2×10^{-5} M in H_2O, rel. ε): 504.5 (0.404), 482.5 (0.402), 404.5 (0.173), 384.5 (0.158), 343.0 (1.00), 268.0 (0.729) (see *Supporting Information*, *Figure S12*). UV-Vis (**Cl_2Rhby**, in about 2×10^{-5} M in 5 M aqueous NaCl, rel. ε): 512.0 (0.387), 485.0 (0.384), 407.5 (0.150), 386.5 (0.120), 346.0 (1.00), 267.5 (0.753) (see *Supporting Information*, *Figure S13*). ESI-MS: 1009.43 (14.6); 1008.42 (52.0); 1007.42 (100, $[M-Cl-H_2O+CH_3OH]^+$, $C_{46}H_{68}N_{10}O_9Rh^+$); 994.41 (3.6); 993.41 (7.6, $[M-Cl]^+$, $C_{45}H_{66}N_{10}O_9Rh^+$) (see *Supporting Information*, *Figure S14*).

Synthesis of Acetylrhodibyrate (**AcRhby**) *from the Chlororhodibyrate Mixture*

A methanolic solution of 1.3 μmol of the roughly 1:1 mixture of the chlororhodibyrates synthesized and isolated through the procedure described above, was dried using an RV. The residue was dissolved in 2.5 ml KP6-buffer to be transferred into a 5 ml flask that was fitted with a 1 mm UV-Vis cell. The orange-yellow solution was degassed through three cycles of freeze, evacuate (HV) and thaw under Ar. Then 5.1 mg (100 equiv.) of $NaBH_4$ were added under inert gas and bubbling as well as a slight color change of the solution to yellow-orange was observed. As a UV-Vis spectrum recorded 28 min after the $NaBH_4$ addition indicated significant adventitious re-oxidation, another portion of 5.1 mg (100 equiv.) $NaBH_4$ was added under inert gas. After 5 min a UV-Vis spectrum indicated reduction with formation of a Rh(I)-corrin (see *Supporting Information*, *Figure S16*) and 5 min later 40 μl (21.2 μmol, 15.8 equiv.) of a solution of 200 μl acetic acid anhydride in 3.8 ml MeOH, chilled to −20 °C and saturated with Argon was added under inert gas. The solution instantly became light yellow and 3 min after the addition of acetic acid anhydride a UV-Vis spectrum showed the characteristics of an organometallic Rh-corrin. The solution was diluted with 15 ml KP6-buffer to be loaded onto a *RP18* cartridge. The adsorbate was washed with 10 ml KP6-buffer and 20 ml of water and was eluted with 8 ml of MeOH. This solution was evaporated to dryness on an RV and the orange colored residue was dissolved in 5 ml water. HPLC-Analysis indicated a single corrin fraction, which was characterized as **AcRhby** by an ESI-MS spectrum (see *Supporting Information*, *Figure S15*) and UV-Vis quantified as about 1.3 μmol. The **AcRhby** solution was concentrated to 2 ml on an RV at $T<$ 40 °C to give the sample of acetylrhodibyrate (**AcRhby**) directly used for the synthesis of **AcRhbl**. UV-Vis ($c\approx1.7\times10^{-4}$ M, H_2O, rel. ε): 481.0 (0.422), 462.0 (0.415), 410.0 (0.178), 398.0 (0.125), 336.5 (1.00), 288.5 (0.476), 265.5 (0.514), 241.5 (0.410) (see *Supporting Information*, *Figure S19*). ^{1}H-NMR (700 MHz, 298 K, D_2O, $c=2$ mm): 0.74 (*s*, 3 H, H_3C2 L); 1.18 (*s*, 3 H, H_3C12B); 1.20 (*s*, 3 H, H_3C1 A); 1.33 (*s*, 3 H, H_3C17B); 1.51 (*s*, 3 H, H_3C2 A); 1.58 (*s*, 3 H, H_3C12 A); 1.73 (*s*, 3 H, H_3C7 A); superimposed by 1.00–1.80 (*m*, in total *ca.* 38 H); 2.43/2.50 (2*s*, 6 H, H_3C51, H_3C151); 2.69 (*m*, 4 H); superimposed by 1.80–2.90 (*m*, in total *ca.* 46 H); 2.98 (*m*, 1 H, HC18); 3.55 (*m-doublett*oid, 1 H, HC13); 3.71 (*m-triplett*oid, 1 H, HC8); 3.93 (*d*, $J=9.6$, 1 H, HC3); 4.09 (*d*, $J=11.7$, 1 H, HC19); superimposed by 2.90–4.40 (*m*, in total *ca.* 13 H); 6.42 (*s*, 1 H, HC10); tentative signal assignment; minor signals of unidentified impurities are not listed (see *Supporting Information*, *Figure S20*). ESI-MS: 1021.42 (16.6); 1020.42 (55.9); 1019.42 (100, $[M+H]^+$, $C_{47}H_{68}N_{10}O_9Rh^+$) (see *Supporting Information*, *Figure S15*).

Synthesis of Acetylrhodibalamin (**AcRhbl**) *from Acetylrhodibyric Acid* (**AcRhby**)

The solution of **AcRhby** from the previous experiment (1.3 μmol) in a 10 ml round bottom flask was concentrated to 2 ml using a RV, and cooled to about 0 °C by an ice bath. Then 1.7 mg (3 equiv.) of B_{12}-nucleotide[2,21] and 1.0 mg (5 equiv.) of HOBt were added and the mixture was stirred to dissolve the solids. Subsequently 5.1 mg (20 equiv.) of EDC·HCl were added, and the solution was stirred at 0 °C for 50 min, when HPLC-analysis of a sample of the mixture indicated roughly 25 % conversion. After a reaction time of one hour, the ice bath was removed and the stirred solution was warmed up to r.t. After 90 min reaction at r.t. roughly 95 % conversion to **AcRhbl** was indicated by HPLC. After a total reaction time of 180 min at r.t., the mixture was diluted with 10 ml KP6-buffer and loaded onto an *RP18* cartridge. The adsorbate was washed with 10 ml KP6-buffer and 10 ml of water and then eluted with 2 ml of MeOH. UV-Vis and HPLC-analysis of the eluate showed **AcRhbl** and B_{12}-nucleotide left (see *Supporting Information*, *Figures S22*). The collected eluate was evaporated on an RV and the residue was re-dissolved in 100 μl of water, for separation through HPLC in two similar sized portions. The fractions of **AcRhbl** were combined, desalted, eluted with 2 ml of MeOH and found pure by HPLC. The solution was evaporated on a RV and the residue was dried applying HV, yielding 1.1 mg of solid **AcRhbl**. The raw **AcRhbl** was dissolved in 80 μl water and 1.0 ml acetone was added slowly in small portions under mixing giving a slightly turbid mixture. Upon storage at r.t. for 15 min, first crystals began to form. The crystallization was completed overnight in a refrigerator at 8 °C. The orange crystals were separated from the mother-liquor, washed twice with about 1 ml of acetone and then dried under high vacuum for 1 hour. 1.1 mg of orange needle-like crystals of **AcRhbl** (0.78 μmol, 58.0 % over all from the chlororhodibyrate mixture) were obtained, characterized by the set of spectra displayed aboveand in the *Supporting Information*, *S20*. UV-Vis ($c = 5.23 \times 10^{-5}$ M, H_2O): 502.5 (3.96), 482.5 (3.93), 415.0 (3.53), 392.5 (3.44), 344.0 (4.33), 289.0 (4.14), 280.5 (4.16), 268.5 (4.15), 249.0 (4.10) (see *Figure 2,A*). ESI-MS: 1456.52 (5.5); 1455.52 (11.4); 1454.52 (15.1, $[M+K]^+$); 1440.55 (31.5); 1439.55 (79.0); 1438.54 (100, $[M+Na]^+$); 1418.57 (10.8); 1417.56 (25.4); 1416.56 (32.8), $[M+H]^+$, $C_{64}H_{92}N_{13}O_{15}PRh^+$) (see *Supporting Information*, *Figure S27*). ^{1}H-NMR (700 MHz, 298 K, KP6-buffer (in H_2O)/D_2O 9:1, $c = 2 \times 10^{-3}$ M, see *Figure 4*; atom numbering, see *Figure 12*). 0.50 (*s*, 3 H, H_3C1 A); 0.77 (*s*, 3 H, H_3C2 L); 0.85–095 (*m*, 1 H, H_AC81); 1.00–1.04 (*m*, 1 H, H_AC82); 1.12 (*d*, *J* = 6.4, 3 H, H_2C177); 1.23 (*s*, 3 H, H_3C12B); 1.28 (*s*, 3 H, H_3C17B); 1.35 (*s*, 3 H, H_3C2 A); 1.46 (*s*, 3 H, H_3C12 A); 1.50–1.56 (*m*, 1 H, H_BC82); 1.79 (*s*, 3 H, H_3C7 A); 1.78–1.83 (*m*, 1 H, H_AC172); 1.80–1.86 (*m*, 1 H, H_BC81); 1.9–2.2 (*m*, in total about 12 H, encompassing 1.96–2.02 (*m*, H_AC131 and H_AC31)); 2.01 (*d*, *J* = 15.0 Hz, H_AC71); 2.04–2.08 (*m*, H_BC172 and H_BC31); 2.09–2.13 (*m*, H_BC131); 2.11 (*s*, 3 H, HC11 N); 2.14 (*s*, 3 H, HC10 N); 2.26 (*d*, *J* = 14.1, 1 H, H_AC21); 2.4–2.65 (*m*, in total about 15 H, encompassing 2.41 (*dd*, *J* = 4.4, 15.7, H_AC171)); 2.42–2.46 (*m*, H_AC32); 2.45 (*d*, *J* = 14.1, H_BC21); 2.47–2.51 (*m*, H_BC32); 2.51 (*dd*, *J* = 4.4/15.7, 1 H, H_BC171); 2.55 (*d*, *J* = 15.0 Hz, 1 H, H_BC71); 2.55–2.60 (*m*, H_AC181); 2.59 (*s*, 3 H, H_3C151); 2.60 (*s*, 3 H, H_3C51); 2.58–2.62 (*m*, HC132); 2.66 (*d*, *J* = 8.2, 1 H, H_BC181); 2.73–2.77 (*m*, 1 H, HC18); 2.98–3.02 (*m*, 1 H, H_AC175); 3.41 (*d*, *J* = 11.6, 1 H, HC13); 3.45–3.49 (*m*, 1 H, H_BC175); 3.59 (*dd*, *J* = 5.6/10.2, 1 H, HC8); 3.65/3.81 (*AB*-system, $J_{AB} = 13.3$, $J_{AX} =$

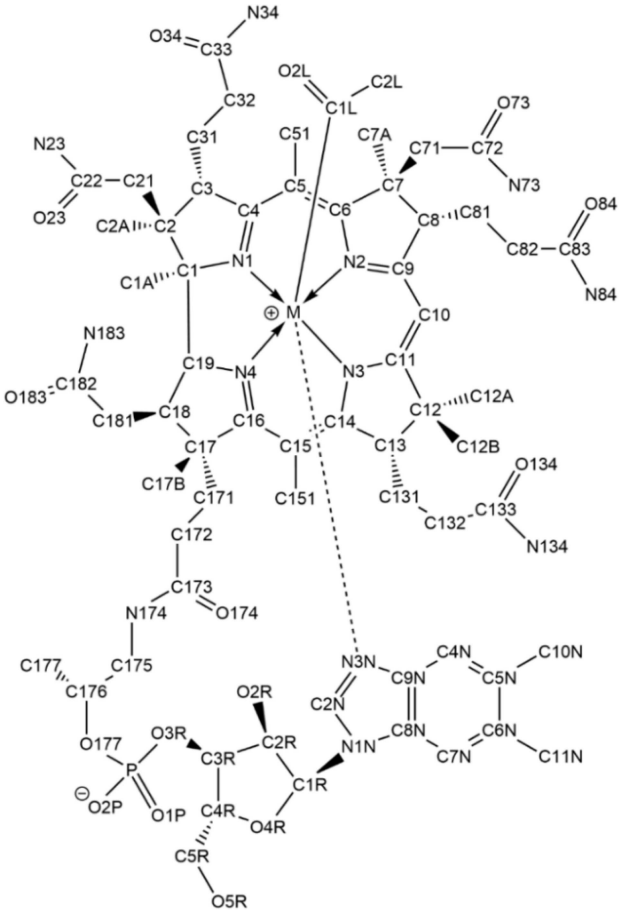

Figure 12. Atom numbering used here for **AcRhbl** (M=Rh(III)) and **AcCbl** (M=Co(III)).

3.7, 2 H, H_2C5R); 3.96–4.00 (*m*, 1 H, HC4R); 4.03 (*d*, *J* = 11.0 Hz, 1 H, HC3); 4.05 (*d*, *J* = 12.2, 1 H, HC19); 4.07–4.12 (*m*, 1 H, HC2R); 4.22–4.27 (*m*, 1 H, HC176); 4.57–4.61 (*m*, 1 H, HC3R); 6.02 (*s*, 1 H, H_EN84); 6.06 (*s*, 1 H, HC4 N); 6.09 (*d*, *J* = 6.1, 1 H, HC1R); 6.11 (*s*, 1 H, HC10); 6.24 (*s*, 1 H, H_ZN84); 6.56 (*s*, 1 H, HC2 N); 6.78 (*s*, 1 H, H_EN34); 6.92 (*s*, 1 H, H_EN134); 6.94 (*s*, 1 H, H_EN184); 6.98 (*s*, 1 H, H_EN23); 7.03 (*s*, 1 H, HC7 N); 7.51 (*s*, 2 H, H_ZN73 + H_ZN34); 7.60 (*s*, 1 H, H_ZN23); 7.67 (*s*, 1 H, H_ZN134); 7.80 (*s*, 1 H, H_ZN183); 8.12 (*t*, *J* = 6.2, 1 H, HN174) (see *Figure 3* and *Supporting Information*, *Tables S6* and *S7*).

Exploratory Photo-Decomposition of **AcCbl** *and* **AcRhbl**

Samples of **AcCbl** and **AcRhbl**, dissolved in H_2O to similar optical densities < 0.3 in aerated 1 mm UV/Vis-absorbance cells, were exposed to direct sunlight on the lab bench. Photolysis of **AcCbl** was practically complete after 20 min, furnishing a red solution of aquo-Cbl, from deacylation. The photolysis with **AcRhbl** was still incomplete after 9 h, according to an analysis of the solution by HPLC. Its yellow main photoproduct had formally added a dioxygen molecule, providing no evidence for de-acylation of **AcRhbl** (see *Supporting Information*, and *Figures S28–S32*).

Exploratory Studies of Biological Activity of **AcRhbl**

The biological activity of **AcRhbl** was investigated by the use of a bioassay, using a *Salmonella enterica* B_{12} auxotroph that relies on a B_{12}-dependent methionine synthase for methionine production as previously described.[54] The use of this strain on a plate-based microbiological bioassay allows not only for the quantitative detection of cobalamin by relating the size of growth circles around an application point on the *Salmonella*-embedded agar, but also allows for the determination of inhibitory molecules by either mixing with specific quantities of cyanocobalamin (**CNCbl**), producing reduced growth circles, or by looking for zones of inhibition when the inhibitor is placed next to the **CNCbl** application point.[9] In the event, application of **AcRhbl** to the bioassay plate failed to promote any growth by itself and competition experiments with **CNCbl** support the conclusion that **AcRhbl** is actively imported by the bacteria resulting in growth inhibition (for further details see *Supporting Information* and *Figure S48*).

Crystallographic Work

Crystals of **AcCbl** for X-ray crystallography were obtained upon slow addition of about 1 ml MeCN to a light protected solution of 1.3 mg of **AcCbl** in about 100 µl of water (until the solution became slightly turbid). The crystals grew upon storage at room temperature (2 h) followed by overnight storage in a refrigerator. Crystals of **AcRhbl** suitable for X-ray crystallography were obtained in a similar way by slow addition of MeCN to a sample of roughly 0.3 mg of **AcRhbl** in about 100 µl of water, till the solution became slightly turbid.

Single-crystals were selected for measurements by a *Bruker D8Quest* diffractometer, equipped with a *Photon 100 CMOS* detector, using molybdenum radiation at temperatures of 183 K for **AcCbl** and 173 K for **AcRhbl**. The crystal structure data for **AcCbl** (CCDC-2217050) and for **AcRhbl** (CCDC-2217051) are available at the Cambridge Data System (see *Supporting Information* for more details).

Quantum Chemical Studies

Initial structures of **AcRhCbl** and **AcCbl** were adapted from the available X-ray crystal structures. These structures were fully optimized with density functional theory (BP86/def2-SVP)[69–71] including empirical dispersion corrections of the D3 type with *Becke–Johnson* damping[72,73] in water. Water was modelled as implicit solvent using the Conductor-Like Screening Model as implemented in Turbomole,[74,75] where the solute is placed in a cavity and the solvent is described by a dielectric continuum, here a permittivity of ε = 78.5 is used. To speed up the calculation time, the resolution-of-identity technique was utilized.[76]

For the conformer search, a pre-final version of the crystal structure served as input structure. The structures calculated starting from the pre-final or the final crystal structures of **AcRhCbl** and **AcCbl** were rather similar: the major difference was the orientation of the nucleotide loop. An overlay of the two structures showed that the geometries at the upper face of the corrin were almost identical (see *Supporting Information*, *Figures S43–S44*). To generate the conformers, the orientation of the acetyl group with respect to the corrin ring, that is the dihedral between N1–M–C1-L–O2-L, was modified by increments of 15°. Each resulting structure was partially optimized with the respective dihedral angle being kept fixed. Final single

point energies on the partially optimized structures were calculated with the range-separated hybrid functional ωB97xd[77] in conjunction with the triple-zeta basis set def2-TZVP[71] and water treated by an implicit solvent model.

All of the above calculations were performed with Turbomole 7.5.[78] (TURBOMOLE V7.5 2020, a development of University of Karlsruhe and Forschungszentrum Karlsruhe GmbH, 1989–2007, TURBOMOLE GmbH, since 2007; available from http://www.turbomole.com). To visualize non-covalent interactions, the approach of *Johnson et al.*[36] was used (see *Supporting Information* for details).

Acknowledgements

The authors thank *Thomas Müller* for mass spectral and Christoph Kreutz for NMR measurements. We are grateful to the *Austrian Science Fund* (FWF) for financial support to *B. K.* (project P 33059) and to *M. P.* (project P 33528) and to the Biotechnology & Biological Sciences Research Council (BBSRC) (project numbers BB/S002197/1 and BB/X001946/1) to *M. J. W.*

Data Availability Statement

The data that support the findings of this study are available in the *Supporting Information* of this article. Cartesian coordinates of all structures are deposited at Zenodo with the DOI: 10.5281/zenodo.7541090.

Author Contribution Statement

B .K., *M. P.* and *M. J. W.* conceived the project. *M. W.*, *C. K.* and *E. D.* synthesized and isolated B_{12}-compounds, directed by *B .K.* and *M. J. W.*; *M. W.* and *C. K.* designed and performed spectral analyses; *K. W.* determined crystal structures; *M. P.* designed and performed the computational studies; *M. D. P.* and *M. J. W.* investigated biological activity; *M. P.*, *B .K.* and *M. J. W.* acquired funding. *B .K.*, *M. W.* and *M. P.* wrote the main draft. All authors read and provided input to the final manuscript.

References

[1] D. C. Hodgkin, J. Kamper, M. Mackay, J. Pickworth, K. N. Trueblood, J. G. White, 'Structure of Vitamin-B_{12}', *Nature* **1956**, *178*, 64–66.
[2] A. Eschenmoser, 'Vitamin-B_{12}: Experiments Concerning the Origin of Its Molecular-Structure', *Angew. Chem. Int. Ed.* **1988**, *27*, 5–39.
[3] B. Kräutler, B. Puffer, 'Vitamin B_{12}-Derivatives: Organometallic Catalysts, Cofactors and Ligands of Bio-Macromolecules', in 'Handbook of Porphyrin Science', Vol. 25, Eds. K. M. Kadish, K. M. Smith, R. Guilard, World Scientific, Singapore, 2012, pp. 131–263.
[4] D. A. Bryant, C. N. Hunter, M. J. Warren, 'Biosynthesis of the modified tetrapyrroles–the pigments of life', *J. Biol. Chem.* **2020**, *295*, 6888–6925.
[5] J. M. Pratt, 'Inorganic Chemistry of Vitamin B_{12}', Academic Press, New York, **1972**.
[6] N. J. Lewis, R. Nussberger, B. Kräutler, A. Eschenmoser, '5,15-Bisnorcobester: an Unexpected Mode of Formation', *Angew. Chem. Int. Ed.* **1983**, *22*, 736–737.
[7] C. Kieninger, E. Deery, A. D. Lawrence, M. Podewitz, K. Wurst, E. Nemoto-Smith, F. J. Widner, J. A. Baker, S. Jockusch, C. R. Kreutz, K. R. Liedl, K. Gruber, M. J. Warren, B. Kräutler, 'The Hydrogenobyric Acid Structure Reveals the Corrin Ligand as an Entatic State Module Empowering B_{12} Cofactors for Catalysis', *Angew. Chem. Int. Ed.* **2019**, *58*, 10756–10760.
[8] J. M. Pratt, 'Electronic Structure and Spectra of B 12: From Trans Effects to Protein Conformation', in 'Chemistry and Biochemistry of B_{12}', Ed. R. Banerjee, John Wiley & Sons, 1999, pp. 73–112.
[9] F. J. Widner, A. D. Lawrence, E. Deery, D. Heldt, S. Frank, K. Gruber, K. Wurst, M. J. Warren, B. Kräutler, 'Total Synthesis, Structure, and Biological Activity of Adenosylrhodibalamin, the Non-Natural Rhodium Homologue of Coenzyme B_{12}', *Angew. Chem. Int. Ed.* **2016**, *55*, 11281–11286.
[10] C. Kieninger, J. A. Baker, M. Podewitz, K. Wurst, S. Jockusch, A. D. Lawrence, E. Deery, K. Gruber, K. R. Liedl, M. J. Warren, B. Kräutler, 'Zinc Substitution of Cobalt in Vitamin B_{12}: Zincobyric acid and Zincobalamin as Luminescent Structural B_{12}-Mimics', *Angew. Chem. Int. Ed.* **2019**, *58*, 14568–14572.
[11] C. Kieninger, K. Wurst, M. Podewitz, M. Stanley, E. Deery, A. D. Lawrence, K. R. Liedl, M. J. Warren, B. Kräutler, 'Replacement of the Cobalt-Center of Vitamin B_{12} by Nickel: Nibalamin and Nibyric Acid Prepared from Metal-Free B_{12} Ligands Hydrogenobalamin and Hydrogenobyric Acid', *Angew. Chem. Int. Ed.* **2020**, *59*, 20129–20136.
[12] F. J. Widner, C. Kieninger, K. Wurst, E. Deery, M. J. Warren, B. Kräutler, 'Synthesis, Spectral Characterization and Crystal Structure of Chlororhodibalamin: A Synthesis Platform for Rhodium Analogues of Vitamin B_{12} and for Rh-Based Antivitamins B_{12}', *Synthesis* **2021**, *53*, 332–337.
[13] B. Kräutler, 'Antivitamins B_{12} – A Structure- and Reactivity-Based Concept', *Chem. Eur. J.* **2015**, *21*, 11280–11287.
[14] B. Kräutler, 'Antivitamins B_{12} – Some Inaugural Milestones', *Chem. Eur. J.* **2020**, *26*, 15438–15445.
[15] O. Müller, G. Müller, 'Synthesen auf dem Vitamin B12-Gebiet, XIV. Über die Synthese von Corrinoiden mit Kobalt-Kohlenstoff-Bindung', *Biochem. Z.* **1962**, *336*, 299–313.

[16] B. Kräutler, 'Acetyl-cobalamin from Photoinduced Carbonylation of Methyl-Cobalamin', *Helv. Chim. Acta* **1984**, *67*, 1053–1059.

[17] K. Bernhauer, E. Irion, 'Synthesen auf dem Vitamin B12-Gebiet, XVII. Co-acyl-cobalamine und deren Transfer-Reaktionen', *Biochem. Z.* **1964**, *339*, 530–538.

[18] E. L. Smith, L. Mervyn, P. W. Muggleton, A. W. Johnson, N. Shaw, 'Chemical Routes to Coenzyme B_{12} and Analogues', *Ann. N. Y. Acad. Sci.* **1964**, *112*, 565–574.

[19] K. M. McCauley, S. R. Wilson, W. A. van der Donk, 'Characterization of Chlorovinylcobalamin, A Putative Intermediate in Reductive Degradation of Chlorinated Ethylenes', *J. Am. Chem. Soc.* **2003**, *125*, 4410–4411.

[20] M. Ruetz, C. Gherasim, K. Gruber, S. Fedosov, R. Banerjee, B. Kräutler, 'Access to Organometallic Arylcobaltcorrins through Radical Synthesis: 4-Ethylphenylcobalamin, a Potential "Antivitamin B_{12}"', *Angew. Chem. Int. Ed.* **2013**, *52*, 2606–2610.

[21] F. Kreppelt, 'Regioselektive Rekonstituierung von Vitamin B12 durch Nukleotidierung von Cobyrinsäure-Heptakis(cyanmethyl)ester', PhD-thesis, ETH Zürich, doi: 10.3929/ethz-a-000626280, 1991.

[22] F. J. Widner, F. Gstrein, B. Kräutler, 'Partial Synthesis of Coenzyme B_{12} from Cobyric Acid', *Helv. Chim. Acta* **2017**, *100*, e1700170.

[23] B. Kräutler, 'Biological Organometallic Chemistry of Vitamin B_{12}-Derivatives', Chapt. 20 in 'Advances in Bioorganometallic Chemistry', Eds. T. Hirao, T. Moriuchi, Elsevier Inc., Cambridge, 2019, pp. 399–429.

[24] H.-U. Blaser, E.-L. Winnacker, A. Fischli, B. Hardegger, D. Bormann, N. Hashimoto, J. Schossig, R. Keese, A. Eschenmoser, 'Corrin-Syntheses. Part V', *Helv. Chim. Acta* **2015**, *98*, 1845–1920.

[25] V. B. Koppenhagen, F. Wagner, J. J. Pfiffner, 'α-(5,6-Dimethylbenzimidazolyl)rhodibamide and Rhodibinamide, Rhodium Analogs of Vitamin-B_{12} and Cobinamide', *J. Biol. Chem.* **1973**, *248*, 7999–8002.

[26] V. B. Koppenhagen, in 'B_{12}, Vol. 2', Ed. D. Dolphin, John Wiley & Sons, 1982, pp. 105–150.

[27] T. A. Stich, A. J. Brooks, N. R. Buan, T. C. Brunold, 'Spectroscopic and Computational Studies of Co^{3+}-Corrinoids: Spectral and Electronic Properties of the B_{12} Cofactors and Biologically Relevant Precursors', *J. Am. Chem. Soc.* **2003**, *125*, 5897–5914.

[28] P. M. Kozlowski, B. D. Garabato, P. Lodowski, M. Jaworska, 'Photolytic properties of cobalamins: a theoretical perspective', *Dalton Trans.* **2016**, *45*, 4457–4470.

[29] B. Cordero, V. Gómez, A. E. Platero-Prats, M. Revés, J. Echeverría, E. Cremades, F. Barragán, S. Alvarez, 'Covalent radii revisited', *Dalton Trans.* **2008**, 2832–2838.

[30] K. M. McCauley, D. A. Pratt, S. R. Wilson, J. Shey, T. J. Burkey, W. A. van der Donk, 'Properties and Reactivity of Chlorovinylcobalamin and Vinylcobalamin and Their Implications for Vitamin B_{12}-Catalyzed Reductive Dechlorination of Chlorinated Alkenes', *J. Am. Chem. Soc.* **2005**, *127*, 1126–1136.

[31] C. Kratky, R. Waditschatka, C. Angst, J. E. Johansen, J. C. Plaquevent, J. Schreiber, A. Eschenmoser, 'Die Sattelkonformation der hydroporphinoiden Nickel(II)-Komplexe: Struktur, Ursprung und stereochemische Konsequenzen', *Helv. Chim. Acta* **1985**, *68*, 1312–1337.

[32] V. B. Pett, M. N. Liebman, P. Murray-Rust, K. Prasad, J. P. Glusker, 'Conformational Variability of Corrins: Some Methods of Analysis', *J. Am. Chem. Soc.* **1987**, *109*, 3207–3215.

[33] L. Randaccio, S. Geremia, G. Nardin, J. Wuerges, 'X-ray structural chemistry of cobalamins', *Coord. Chem. Rev.* **2006**, *250*, 1332–1350.

[34] K. L. Brown, 'Chemistry and Enzymology of Vitamin B_{12}', *Chem. Rev.* **2005**, *105*, 2075–2150.

[35] B. Kräutler, C. Kratky, 'X-ray Crystallography of B_12', in 'Chemistry and Biochemistry of B_{12}', Ed. R. Banerjee, John Wiley & Sons, New York, Chichester, 1999, pp. 9–41.

[36] E. R. Johnson, S. Keinan, P. Mori-Sánchez, J. Contreras-García, A. J. Cohen, W. Yang, 'Revealing Noncovalent Interactions', *J. Am. Chem. Soc.* **2010**, *132*, 6498–6506.

[37] J. Contreras-García, E. R. Johnson, S. Keinan, R. Chaudret, J.-P. Piquemal, D. N. Beratan, W. Yang, 'NCIPLOT: A Program for Plotting Noncovalent Interaction Regions', *J. Chem. Theory Comput.* **2011**, *7*, 625–632.

[38] C. Brenig, M. Ruetz, C. Kieninger, K. Wurst, B. Kräutler, 'Alpha- and Beta-Diastereoisomers of Phenylcobalamin from Cobalt-Arylation with Diphenyliodonium Chloride', *Chem. Eur. J.* **2017**, *23*, 9726–9731.

[39] G. Holze, H. H. Inhoffen, 'The First Chemical Partial Synthesis of the Nickel-Complex of a Cobyrinic Acid-Derivative', *Angew. Chem. Int. Ed.* **1985**, *24*, 867–869.

[40] C. Brenig, L. Prieto, R. Oetterli, F. Zelder, 'A Nickel(II)-Containing Vitamin B_{12} Derivative with a Cofactor-F430-type π-System', *Angew. Chem. Int. Ed.* **2018**, *57*, 16308–16312.

[41] T. C. Brunold, K. S. Conrad, M. D. Liptak, K. Park, 'Spectroscopically validated density functional theory studies of the B_{12} cofactors and their interactions with enzyme active sites', *Coord. Chem. Rev.* **2009**, *253*, 779–794.

[42] A. S. Rury, T. E. Wiley, R. J. Sension, 'Energy Cascades, Excited State Dynamics, and Photochemistry in Cob(III)alamins and Ferric Porphyrins', *Acc. Chem. Res.* **2015**, *48*, 860–867.

[43] H. Lebertz, H. Simon, L. F. Courtney, S. J. Benkovic, L. D. Zydowsky, K. Lee, H. G. Floss, 'Stereochemistry of Acetic-Acid Formation from 5-Methyltetrahydrofolate by *Clostridium thermoaceticum*', *J. Am. Chem. Soc.* **1987**, *109*, 3173–3174.

[44] U. Holder, D.-E. Schmidt, E. Stupperich, G. Fuchs, 'Autotrophic synthesis of activated acetic acid from two carbon dioxide in *Methanobacterium thermoautotrophicum*. III. Evidence for common one-carbon precursor pool and the role of corrinoid', *Arch. Microbiol.* **1985**, *141*, 229–238.

[45] H. G. Wood, S. W. Ragsdale, E. Pezacka, 'The acetyl-CoA pathway: a newly discovered pathway of autotrophic growth', *Trends Biochem. Sci.* **1986**, *11*, 14–18.

[46] J. G. Zeikus, R. Kerby, J. A. Krzycki, 'Single-Carbon Chemistry of Acetogenic and Methanogenic Bacteria', *Science* **1985**, *227*, 1167–1173.

[47] S. W. Ragsdale, 'Metals and Their Scaffolds to Promote Difficult Enzymatic Reactions', *Chem. Rev.* **2006**, *106*, 3317–3337.

[48] S. W. Ragsdale, E. Pierce, 'Acetogenesis and the Wood–Ljungdahl pathway of CO_2 fixation', *Biochim. Biophys. Acta Proteins Proteomics* **2008**, *1784*, 1873–1898.

[49] L. Walder, R. Orlinski, 'Mechanism of the Light-Assisted Nucleophilic Acylation of Activated Olefins Catalyzed by Vitamin B_{12}', *Organometallics* **1987**, *6*, 1606–1613.
[50] J. Radebner, A. Eibel, M. Leypold, C. Gorsche, L. Schuh, R. Fischer, A. Torvisco, D. Neshchadin, R. Geier, N. Moszner, R. Liska, G. Gescheidt, M. Haas, H. Stueger, 'Tetraacylgermanes: Highly Efficient Photoinitiators for Visible-Light-Induced Free-Radical Polymerization', *Angew. Chem. Int. Ed.* **2017**, *56*, 3103–3107.
[51] B. Kräutler, 'Antivitamins B12', Chapt. 8 in 'Vitamins and Hormones', Vol. 119, Ed. G. Litwack, Academic Press, Cambridge, MA, 2022, pp. 221–240.
[52] W. Friedrich, 'Vitamins', Walter de Gruyter, Berlin, **1988**.
[53] F. Zelder, M. Sonnay, L. Prieto, 'Antivitamins for Medicinal Applications', *ChemBioChem* **2015**, *16*, 1264–1278.
[54] E. Raux, A. Lanois, F. Levillayer, M. J. Warren, E. Brody, A. Rambach, C. Thermes, '*Salmonella typhimurium* cobalamin (vitamin B_{12}) biosynthetic genes: Functional studies in *S. typhimurium* and *Escherichia coli*', *J. Bacteriol.* **1996**, *178*, 753–767.
[55] K. J. Kennedy, F. J. Widner, O. M. Sokolovskaya, L. V. Innocent, R. R. Procknow, K. C. Mok, M. E. Taga, 'Cobalamin Riboswitches Are Broadly Sensitive to Corrinoid Cofactors to Enable an Efficient Gene Regulatory Strategy', *mBio* **2022**, *13*, e01121–22.
[56] A. Nahvi, J. E. Barrick, R. R. Breaker, 'Coenzyme B_{12} riboswitches are widespread genetic control elements in prokaryotes', *Nucl. Acids Res.* **2004**, *32*, 143–150.
[57] V. B. Koppenhagen, B. Elsenhans, F. Wagner, J. J. Pfiffner, 'Methylrhodibalamin and 5′-Deoxyadenosylrhodibalamin, the Rhodium Analogs of Methylcobalamin and Cobalamin Coenzyme', *J. Biol. Chem.* **1974**, *249*, 6532–6540.
[58] S. N. Fedosov, 'Physiological and Molecular Aspects of Cobalamin Transport', in 'Water Soluble Vitamins', Vol. 56, Ed. O. Stanger, Springer, Dordrecht, 2012, pp. 347–368.
[59] R. Green, L. H. Allen, A.-L. Bjørke-Monsen, A. Brito, J.-L. Gueant, J. W. Miller, A. M. Molloy, E. Nexo, S. Stabler, B.-H. Toh, P. M. Ueland, C. Yajnik, 'Vitamin B_{12} deficiency', *Nat. Rev. Dis. Primers* **2017**, *3*, 17040.
[60] R. Banerjee, H. Gouda, S. Pillay, 'Redox-Linked Coordination Chemistry Directs Vitamin B_{12} Trafficking', *Acc. Chem. Res.* **2021**, *54*, 2003–2013.
[61] C. Bradbeer, 'Cobalamin Transport in Bacteria', in Chemistry and Biochemistry of B_{12}', Ed. R. Banerjee, John Wiley & Sons, New York, 1999, pp. 489–506.
[62] K. Gopinath, A. Moosa, V. Mizrahi, D. F. Warner, 'Vitamin B_{12} metabolism in *Mycobacterium tuberculosis*', *Future Microbiol.* **2013**, *8*, 1405–1418.
[63] K. E. Helliwell, A. D. Lawrence, A. Holzer, U. J. Kudahl, S. Sasso, B. Kräutler, D. J. Scanlan, M. J. Warren, A. G. Smith, 'Cyanobacteria and Eukaryotic Algae Use Different Chemical Variants of Vitamin B_{12}', *Curr. Biol.* **2016**, *26*, 999–1008.
[64] K. Bernhauer, O. Müller, F. Wagner, 'Neuere chemische und biochemische Entwicklungen auf dem Vitamin-B_{12}-Gebiet', *Angew. Chem.* **1963**, *75*, 1145.
[65] G. Li, F. F. Zhang, N. Pi, H. L. Chen, S. Y. Zhang, K. S. Chan, 'Determination of Rh–C Bond Dissociation Energy in Methyl(porphyrinato)rhodium(III) Complexes: a New Application of Photoacoustic Calorimetry', *Chem. Lett.* **2001**, *30*, 284–285.
[66] M. Ruetz, A. Shanmuganathan, C. Gherasim, A. Karasik, R. Salchner, C. Kieninger, K. Wurst, R. Banerjee, M. Koutmos, B. Kräutler, 'Antivitamin B_{12} Inhibition of the Human B_{12}-Processing Enzyme CblC: Crystal Structure of an Inactive Ternary Complex with Glutathione as the Cosubstrate', *Angew. Chem. Int. Ed.* **2017**, *56*, 7387–7392.
[67] M. Ruetz, M. Koutmos, B. Kräutler, 'Antivitamins B_{12}: Synthesis and Application as Inhibitory Ligand of the B_{12}-Tailoring Enzyme CblC', Chapt. 8 in 'Coenzyme B_{12} Enzymes', Vol. 668, Ed. N. Marsh, in 'Methods in Enzymology', Academic Press, 2022, pp. 157–178.
[68] L. Hannibal, P. M. DiBello, M. Yu, A. Miller, S. Wang, B. Willard, D. S. Rosenblatt, D. W. Jacobsen, 'The MMACHC proteome: Hallmarks of functional cobalamin deficiency in humans', *Mol. Genet. Metab.* **2011**, *103*, 226–239.
[69] A. D. Becke, 'Density-functional exchange-energy approximation with correct asymptotic-behavior', *Phys. Rev. A* **1988**, *38*, 3098–3100.
[70] J. P. Perdew, 'Density-functional approximation for the correlation energy of the inhomogeneous electron gas', *Phys. Rev. B* **1986**, *33*, 8822–8824.
[71] F. Weigend, R. Ahlrichs, 'Balanced basis sets of split valence, triple zeta valence and quadruple zeta valence quality for H to Rn: Design and assessment of accuracy', *Phys. Chem. Chem. Phys.* **2005**, *7*, 3297–3305.
[72] S. Grimme, J. Antony, S. Ehrlich, H. Krieg, 'A consistent and accurate *ab initio* parametrization of density functional dispersion correction (DFT–D) for the 94 elements H–Pu', *J. Chem. Phys.* **2010**, *132*, 154104.
[73] S. Grimme, S. Ehrlich, L. Goerigk, 'Effect of the damping function in dispersion corrected density functional theory', *J. Comput. Chem.* **2011**, *32*, 1456–1465.
[74] A. Schäfer, A. Klamt, D. Sattel, J. C. W. Lohrenz, F. Eckert, 'COSMO Implementation in TURBOMOLE: Extension of an efficient quantum chemical code towards liquid systems', *Phys. Chem. Chem. Phys.* **2000**, *2*, 2187–2193.
[75] A. Klamt, G. Schüürmann, 'COSMO: a new approach to dielectric screening in solvents with explicit expressions for the screening energy and its gradient', *J. Chem. Soc. Perkin Trans. 2* **1993**, 799–805.
[76] K. Eichkorn, O. Treutler, H. Öhm, M. Häser, R. Ahlrichs, 'Auxiliary basis sets to approximate Coulomb potentials', *Chem. Phys. Lett.* **1995**, *240*, 283–289.
[77] J.-D. Chai, M. Head-Gordon, 'Long-range corrected hybrid density functionals with damped atom–atom dispersion corrections', *Phys. Chem. Chem. Phys.* **2008**, *10*, 6615–6620.
[78] S. G. Balasubramani, G. P. Chen, S. Coriani, M. Diedenhofen, M. S. Frank, Y. J. Franzke, F. Furche, R. Grotjahn, M. E. Harding, C. Hättig, A. Hellweg, B. Helmich-Paris, C. Holzer, U. Huniar, M. Kaupp, A. M. Khah, S. K. Khani, T. Müller, F. Mack, B. D. Nguyen, S. M. Parker, E. Perlt, D. Rappoport, K. Reiter, S. Roy, M. Rückert, G. Schmitz, M. Sierka, E. Tapavicza, D. P. Tew, C. van Wüllen, V. K. Voora, F. Weigend, A. Wodyński, J. M. Yu, 'TURBOMOLE: Modular program suite for *ab initio* quantum-chemical and condensed-matter simulations', *J. Chem. Phys.* **2020**, *152*, 184107.

Received November 9, 2022
Accepted December 12, 2022

